HIGH POWER BEARINGLESS SLICE MOTOR (3-4kW) FOR BEARINGLESS CANNED PUMPS

Pascal Nang Bösch
Swiss Federal Institute of Technology (ETH),
Laboratory for Electrical Engineering Design (EEK)
Technoparkstrasse 1, CH-8005 Zurich, Switzerland
boesch@eek.ee.ethz.ch

Dr. Natale Barletta
Levitronix GmbH,
Technoparkstrasse 1, CH-8005 Zurich, Switzerland
barletta@levitronix.com

ABSTRACT
In the manufacturing industry many processes involve chemical liquids. There are processes like etching, stripping, cleaning or polishing involving aggressive liquid chemicals. Depending on the process all kinds of acid, organic solvents and bases are used and have to be pumped through the fabrication tools. In these wet processes, pumps are one of the most critical parts. Especially in the semiconductor industry the quality of the processes highly depends on the purity of the chemicals. Therefore process pumps have to fulfill high requirements on chemical resistance, purity and reliability, which pneumatically driven bellows or diaphragm pumps satisfy. However, these pumps have considerable disadvantages such as: pulsating flow, mechanical wear, short life time and low energy efficiency. Bearingless centrifugal pump systems can be the solution for these problems.

In this paper a new 3-phase bearingless permanent magnet slice motor is presented. This bearingless slice motor has a mechanical power of up to 4kW and is used in a centrifugal pump application. A typical application area for this power range is the semiconductor and the chemical industry. In delivery applications high purity pump systems with an operating flow of up to 150l/min and an operating pressure of 4,5bar are required. Such an operating point assumes a mechanical drive power of about 3 – 4kW. This development has been done in close collaboration with the company Levitronix in Switzerland.

INTRODUCTION
Normally, two radial bearings are needed for the full stabilisation of five spatial degrees of freedom of a rotor. Therefore in a bearingless motor design two motor/bearing parts are usually required. Such a motor construction becomes rather long. For the levitation and driving of slice shaped rotors, as can be found with centrifugal pumps, this arrangement is not ideal. The idea of the bearingless slice motor is to choose the length of the rotor small compared to its diameter. In this case it is possible to stabilise three spatial degrees of freedom passively. Only one active radial bearing is needed. Active control of the rotation and the radial position of the motor slice is assured by the principle of the bearingless motor. With this concept, a simple solution for a centrifugal pump is possible. Figure 1 shows the basic arrangement of a bearingless slice motor pump of temple design.

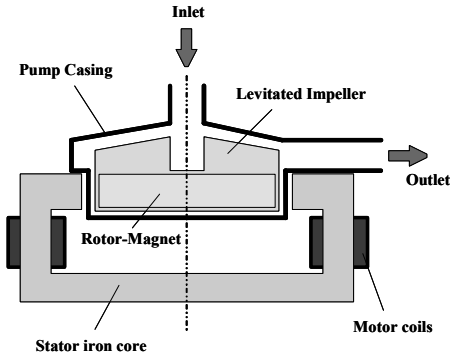

FIGURE 1: Principle of bearingless slice motor pump

The functional principle of the passive stabilization is shown in Figure 2. Figure 2a.) shows an axial displacement of the slice rotor. The displacement results in attractive magnetic forces, which act against the displacement and therefore stabilize the axial position of the

rotor. Figure 2b.) shows a tilting of the slice rotor, which results in a torque against the tilt.

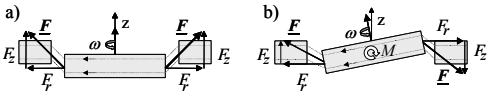

FIGURE 2: Passive stabilization of slice rotor

In the existing bearingless slice motors the rotor is a diametrically magnetized permanent magnet slice (one pole pair). The used high-energy magnet material (NdFeB) allows air gaps of 4mm and more. As shown in Figure 3, the magnetic circuit of the temple motor is closed by a stator back iron at the bottom of the motor. Active control of radial position and the rotation of the slice rotor are assured by the currents in the bearing and drive coils of the bearingless motor. The existing, bearingless motor with eight slots, possesses two bearing phases and two drive phases. To supply all four motor phases, a frequency converter with altogether eight half bridges is needed.

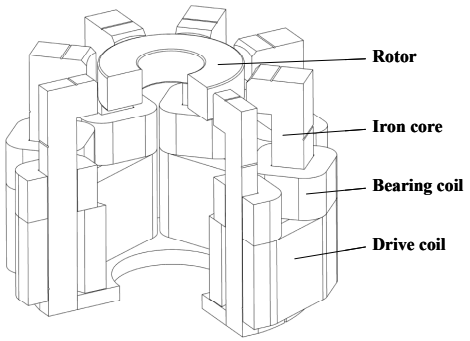

FIGURE 3: Bearingless slice motor of temple design

The technology of low power bearingless 2-phase slice motors with a mechanical power of up to 1.2kW is already mature [2], [3], [4], [6], [7]. Bearingless centrifugal pump systems have been applied in different industries, like the semiconductor industry, the chemical processing industry and for medical applications. However, no bearingless slice motors with a mechanical power of more than 1.2kW with a practical industrial application have been ever produced.

CONFIGURATION ANALYSIS

An important point for a power enhancement of bearingless pump systems is to reduce the manufacturing costs. Bearingless motors with only six slots could cut the manufacturing costs of the motor and the electronic unit significantly. For this reason bearingless slice motors with six slots and different rotor pole pair numbers will be analyzed and discussed.

Magnetic forces in a bearingless slice motor are based on Maxwell and Lorenz forces according to equation (1) and (2).

$$dF_M = \frac{B^2 \cdot dA}{2 \cdot \mu_0} \tag{1}$$

$$dF_L = B \cdot I \cdot dl\,, \qquad (d\underline{l} \perp \underline{B}) \tag{2}$$

The condition for the realization of a magnetic bearing in a bearingless slice motor is given by equation (2).

$$p_2 = p_1 \pm 1 \tag{3}$$

p_1 ... pole pair number of the rotor
p_2 ... pole pair number of the bearing

Radial bearing forces and drive torque of a bearingless slice motor can be approximately calculated with the following equations which are affiliated in [5].

$$F_s = -l_s \cdot r_s \cdot \int_{-\pi}^{\pi} \begin{bmatrix} \cos\alpha & -\sin\alpha & 0 \\ \sin\alpha & \cos\alpha & 0 \\ 0 & 0 & 1 \end{bmatrix} \cdot \begin{bmatrix} \frac{B_{1n}^2}{2 \cdot \mu_0} \\ B_{1n} \cdot A_s \\ 0 \end{bmatrix} \cdot d\alpha \tag{4}$$

α ... rotor angle
B_{1n} ... normal component of flux density
A_s ... current density
l_s ... stator lenght
r_s ... stator radius

$$M_s = -l_s \cdot r_s^2 \cdot \int_{-\pi}^{\pi} B_{1n} \cdot A_s \cdot d\alpha \tag{5}$$

The following simulations are based on the equations (4), (5) and were made in close collaboration with *LCM (Linz Center of Compe-tence in Mechatronics, Austria)*. With a limited maximal bearing current the bearing force in a fixed radial direction was calculated for different rotor angles.

Bearingless Motor with a one pole pair permanent magnet slice rotor

In Table 1 and Figure 4 the data and the functional principle of the bearingless motor with six slots and a one pole pair permanent magnet slice rotor are shown. The field distribution at the outer radius of the permanent magnet is sinusoidal.

Description	*Symbol*	*Value*
Bearing coil angle	α_{pb}	40°
Drive coil angle	α_{pd}	40°
Bearing phase number	m_b	3
Drive phase number	m_d	3
Pairs of poles (bearing)	p_2	2
Pairs of poles (drive)	p_1	1
Current change (bearing)	dl/dφ	0,032

TABLE 1: 2-pole motor configuration

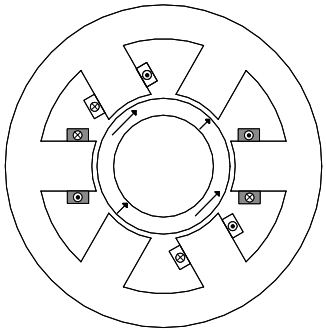

FIGURE 4: 2-pole motor configuration

Figure 5 shows the maximal bearing force in a fixed radial direction with different rotor angles. According to the results in Figure 5, the magnetic bearing with $p_2=p_1+1$ is easy to realize. This configuration will be capable of being put into practice.

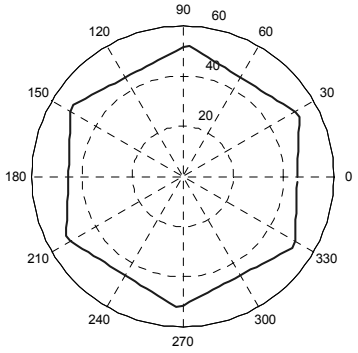

FIGURE 5: Bearing force in a fixed radial direction versus rotor angle

Bearingless slice Motor with a two pole pair permanent magnet slice rotor

In Table 2 and Figure 6 the data and the functional principle of the bearingless motor with six slots and a two pole pair permanent magnet slice rotor are shown. The field distribution at the outer radius of the permanent magnet is also sinusoidal.

Description	*Symbol*	*Value*
Bearing coil angle	α_{pb}	40°
Drive coil angle	α_{pd}	40°
Bearing phase number	m_b	3
Drive phase number	m_d	3
Pairs of poles (bearing)	p_2	1
Pairs of poles (drive)	p_1	2
Current change (bearing)	dl/dφ	0,19

TABLE 2: 4-pole motor configuration

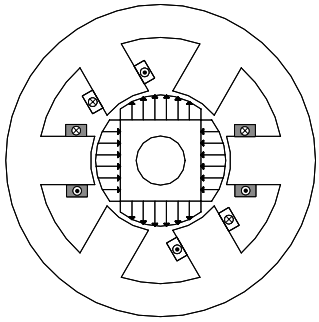

FIGURE 6: 4-pole motor configuration

Figure 7 shows the maximal bearing force in a fixed radial direction with different rotor angle. The big force incursions, makes a realization of a magnetic bearing with this configuration impossible. The basic problem is that in this configuration the Maxwell forces and the Lorenz forces are oppositely aligned. Therefore a magnetic bearing with $p_2=p_1-1$ is difficult to realize [1] and will not be further discussed in this paper.

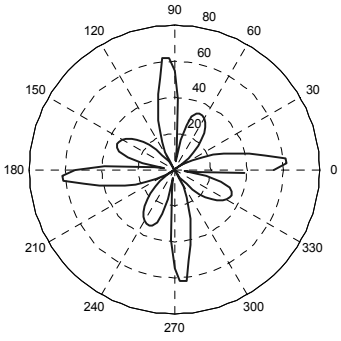

FIGURE 7: Bearing force in a fixed radial direction versus rotor angle

HIGH POWER BEARINGLESS SLICE MOTOR WITH SIX SLOTS

The principal assembly of a 4kW bearingless slice motor with six slots and a diametrically magnetized permanent magnet slice rotor with one pole pair is show in Figure 8. For a better overview only one bearing phase and one drive

phase is wired. I_{1a} indicates the current of a drive phase and I_{2a} the current of a bearing phase. The rotor angle and position are measured with eddy current and Hall sensors which are located between the iron slots.

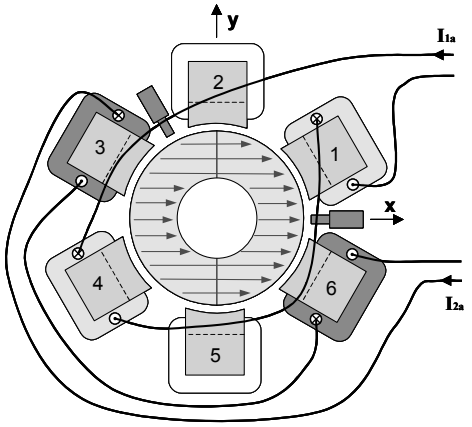

FIGURE 8: Schematic setup of 2-pole bearingless slice motor

In Figure 9 the motor losses, like copper losses of the bearing and drive coils and the iron losses are shown. The losses in Figure 9 refer to the realized bearingless slice motor, with an electrical input power of 3.5kW. A minimum of motor losses will be reached at a rotation speed between 5500 and 7500rpm. This is the rotation speed that is needed to get operating pressures up to 4bar with an impeller diameter of 80mm. If the motor works in an optimal operating point, the total copper losses and the iron losses are of the same dimension. At the rated optimal operating point the motor works with an efficiency of nearly 95%.

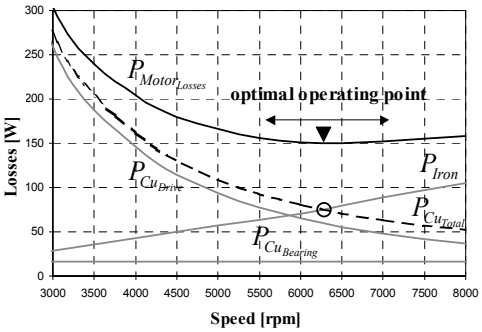

FIGURE 9: Motor losses

$$P_{Motor_{Losses}} = P_{Iron} + P_{Cu_{Drive}} + P_{Cu_{Bearing}} \qquad (6)$$

Picture 1 shows the 4kW bearingless slice motor without casing. It is 230mm high and 200mm in diameter. The protectung cup (black part) prevent damaging of the motor in case of a leaky pump housing.

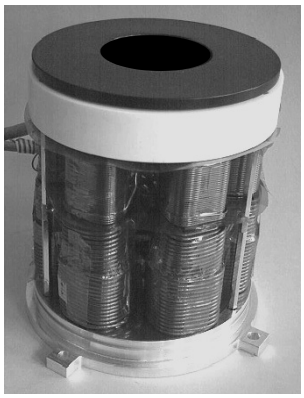

PICTURE 1: 4kW bearingless slice Motor with six slots

FREQUENCY CONVERTER

The realized pump system is controlled by a compact electronic unit. The reduction of the number of slots allows the complexity of the frequency converter to be reduced. Only six power half bridges with a maximal output current of 40A are needed to supply the six phases (3 drive/3 bearing). The power bridges are realized with two integrated three-phase IGBT power bridges by Toshiba. The converter operates with a supply voltage of 3x115...230V AC or 1x208...230V AC. Position, speed and current control loops are realized fully by software in a digital signal processor TMS320F240 by Texas Instruments. The control structure of the bearingless slice motor is based on vector control [7]. Furthermore there are a PLC-interface (Programmable Logic Controller) to the process tool and an RS232 service interface included on the controller board. The electronic unit is inserted in a compact steel casing (210x220x330mm) including a fortified fan cooling. Due to the additional built-in user interface with an alpha-numeric control display, the bearingless pump system can also work as a stand-alone system.

PICTURE 2: 4kW frequency converter

PUMP DESIGN

The dimensioning technique for the impeller blades and the pump housing is already mature and could be taken from [8] and [9]. One of the most important problems is the treatment of the hydrodynamic axial trust in a bearingless centrifugal pump system, which is increasingly disproportionate with the extension of the pump size. The axial force of the passive axial magnetic bearing increases with the power of two by an extension of all pump dimensions and depends approximately linear on the axial deflection. Furthermore the axial stiffness can be slightly increased by increasing the magnetization of the permanent magnet. In contrast to the axial magnet force, the hydrodynamic trust increases with the power of four by an extension of all pump dimensions. On this account any increasing of pump dimensions will be problematical. Figure 10 shows a schematic setup of a bearingless centrifugal pump with the different flows inside the pump. By optimizing the diameter of the pressure compensation holes, the impeller position can be stabilized by influencing the leakage flow and the pressure on the impeller bottom.

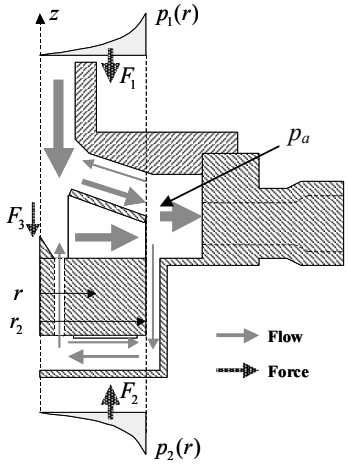

FIGURE 10: Schematic setup of a bearingless centrifugal pump

The condition for a stable axial position of the impeller is that the axial magnet force is equal to the hydrodynamic trust.

$$F_{zhydr} + F_z = F_{zhydr} - k_z \cdot z = 0 \qquad (7)$$

With equation (8) and (9) the pressures on the top and on the bottom of the impeller can be calculated approximately.

$$p_{1,2}(r) = p_a - \omega_{fl1,2}^2 \cdot \rho \cdot \frac{r_2^2 - r^2}{2} \qquad (8)$$

$$\omega_{fl} = \frac{1}{2} \cdot \omega_m \qquad (9)$$

In order that the hydrodynamic thrust can be estimated, all hydrodynamic axial forces must be ascertained. The axial forces F_1 and F_2 can be calculated with the following equation.

$$F_{1,2} = \int_0^{2\pi} \int_{r_i}^{r_2} r \cdot p_{1,2}(r) dr d\varphi \qquad (10)$$

Equation (11) characterize the impact pressure at the pump inlet. ΔV_a specifies the difference of the axial fluid velocities between impeller inlet and outlet.

$$F_3 \approx \rho \cdot Q \cdot \Delta V_a \qquad (11)$$

The hydrodynamic axial thrust can finally be expressed by equation (12).

$$F_{zhyd} = F_2 - F_1 - F_3 \qquad (12)$$

Figure 11 shows a cross section of the bearingless centrifugal pump with a maximal hydraulic power of 950W. The axial impeller balancing is achieved with pressure compensation holes and additional compensation blades on the impeller bottom.

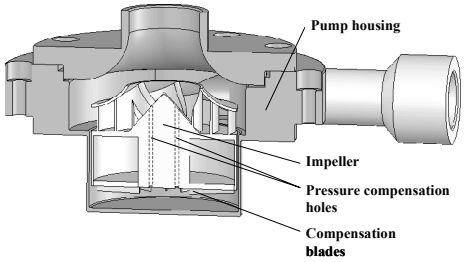

FIGURE 11: Pump housing with impeller

The operating range and the pump parts of the realized bearingless pump are shown in Figure 12 and Picture 3. According to the pressure flow curves, this pump is dedicated for high purity applications with an operating pressure up to 4,5bar and an operating flow up to 170l/min.

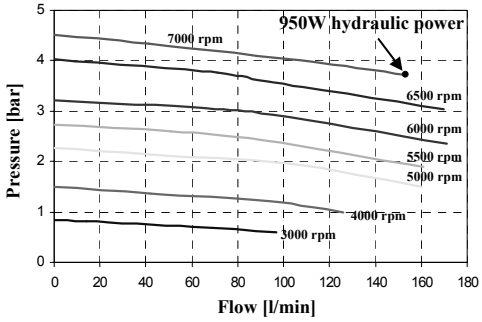

FIGURE 12: Pressure flow curve

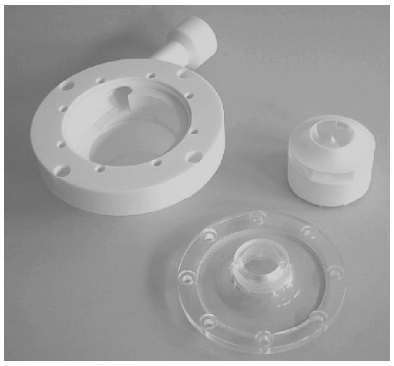

PICTURE 3: Impeller and pump housing parts

BEARINGLESS PUMP

Picture 4 shows the realized 4kW bearingless slice motor and the centrifugal pump, which are 340mm high and 250mm in diameter. On the back of the motor an optional fan cooling module is mounted. Another possibility is to realize water cooling outside or inside the motor. This will be necessary if the motor works a higher power range above 4kW.

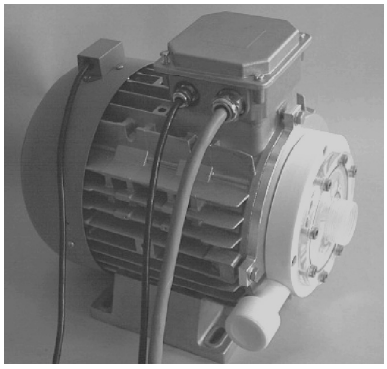

PICTURE 4: 4kW bearingless slice motor pump

SUMMARY

The prototype of a 4kW bearingless pump system is shown in Pictures 2 and 4. It is appropriate for high purity applications in the semiconductor industry and the chemical industry. Because of contact-free bearing there is virtually no generation of particles inside the pump. As the pump principle is rotary, flow and pressure are continuous and can be controlled precisely. By using a bearingless slice motor with only six slots, a cost-effective design of the motor and the electronic unit becomes feasible. Motor, pump and control unit are small in size with regard to the maximal hydraulic power of 950W. This prototype proves that the motor configuration and technology, presented in this paper, allow bearingless slice motors to be produced with a mechanical power of up to 4kW for sophisticated industrial applications.

References

[1] Schöb R., Beiträge zur lagerlosen Asynchronmaschine, Dissertation ETH Zürich, 1993

[2] Barletta N., Der lagerlose Scheibenmotor, Dissertation ETH Zürich, 1998

[3] Neff M., Magnetgelagertes Pumpsystem für die Halbleiterfertigung, Dissertation ETH Zürich, 2003

[4] Neff M., Barletta N., Schöb R., Bearingless Centrifugal Pump for Highly Pure Chemicals, The Eight International Symposium on Magnetic Bearing, Mito, Japan, 2002

[5] Silber S., Beiträge zum lagerlosen Einphasenmotor, Dissertation Johannes Kepler Universität Linz, 2000

[6] Schöb R., Barletta N., Hahn J., The Bearingless Centrifugal Pump - a perfect example of a Mechatronics System, First IFAC-Conference on Mechatronic Systems, Darmstadt, Germany, 2000

[7] Schöb R., Bichsel j., Vector Control of the Bearingless Motor, Fourth International Symposium on Magnetic Bearings, Zürich, 1994

[8] Gülich J., Kreiselpumpen, Springer Verlag, 1999

[9] Neumaier R., Hermetische Pumpen, Verlag und Bildarchiv W.H. Faragallah,